

Influence of Inlet Flow Condition on Turbine Blade Showerhead Film Cooling

Chowdhury N.H.K., Qureshi S.A., Zhang M. and Han J.C.*

*Author for correspondence

Department of Mechanical Engineering

Texas A&M University

College Station, TX 77843, USA

E-mail address: jc-han@tamu.edu

ABSTRACT

This study focuses on the influence of the internal flow condition on turbine blade showerhead region film cooling. The elliptical leading edge model has five rows of film cooling holes with 15 holes each at fixed hole-to-hole spacing of 4-diameter and located along the stagnation line (0°), at $\pm 30^\circ$ and at $\pm 60^\circ$ measured from the stagnation line. Two inlet flow conditions, channel flow, and impinging flow are investigated separately, and the effects of coolant-to-mainstream density ratios ($DR = 1.0, 1.5$ and 2.0) with three different coolant-to-mainstream blowing ratios ($M = 0.5, 1.0$ and 1.5) are tested using pressure sensitive paint measurement technique. Experiments were conducted in a suction type low-speed wind-tunnel facility at a flow Reynolds number around 100,000 based on the oncoming mainstream velocity and leading edge diameter. The mainstream turbulence intensity near the leading edge model is about 7%. Results indicate that overall the impingement inlet configuration provides better film effectiveness for all the DRs. However, the difference is found to be minimum at $M = 0.5$ and 1.0 for heavier density coolant ($DR = 2.0$). Additionally, computational simulations have been performed to understand the flow physics of these two inlet flow configurations using a realizable k -epsilon turbulence model.

NOMENCLATURE

C	Mass fraction
D	Diameter of film cooling hole
I	PSP emission intensity
DR	Coolant-to-mainstream density ratio = ρ_c/ρ_∞
L	Hole length
M	Coolant-to-mainstream blowing ratio = $\rho_c V_c/\rho_\infty V_\infty$
P	Static pressure
s	Surface distance
T	Temperature
Tu	Turbulence intensity
α	Surface angle
η	Film cooling effectiveness
ρ	Density
Θ	dimensionless temperature
Subscript	
∞	Mainstream
aw	Adiabatic wall
blk	Black condition

c	Coolant
mix	Mixture
ref	Reference condition

Acronyms

CCD	Charge Couple Device
GH	Gill Film Hole
HTC	Heat Transfer Coefficient
LE	Leading Edge
PSP	Pressure Sensitive Paint
RKE	Realizable K-epsilon

INTRODUCTION

Gas turbines are used for aircraft propulsion, land-based power generation, and industrial applications. Thermal efficiency and power output of gas turbines increase with increasing turbine inlet temperatures (TIT). Current advanced gas turbines operate at TIT far higher than the yielding point of super alloy material; therefore, turbine blades are cooled by compressor discharge air through the internal cooling passage and external film cooling protection. The leading edge (LE) of a blade is the most critical area that suffers the highest heat load. Typically, a film cooling scheme is employed around the LE by inducing coolant through film cooling holes located on the outer surface of the blade. Coolant air is a precious commodity in gas turbine since it affects the thermal efficiency of the turbine, hence precise estimation of the coolant to be used and an efficient coolant delivery system design are very important.

Blowing ratio (M) is the ratio of coolant mass flux to that of mainstream. Film cooling effectiveness has generally been observed to increase with increasing blowing ratio, however, in the case of a leading edge the effect is different in the stagnation region and the first cooling hole row at $+30^\circ$. Also it is interesting to see the effect of gill film holes (GH) on overall film cooling. As per Falcoz et al. [1] at blowing ratio higher than 1.76, coolant lift-off comes into play and increasing blowing ratio may not have the desired effect subsequently. However, this study only deals with blowing ratios 0.5, 1.0 and 1.5 so that the tipping point has not been observed and for the given range increasing a blowing ratio has a positive impact. Similar results are discussed by Li et al. [2].

Density ratio is the ratio of coolant density to mainstream density. Film cooling effectiveness depends heavily on the density ratio of coolant. In most gas turbines, typical coolant

density ratio is kept at 1.5 to 2.0 [3]. The temperature difference between coolant and mainstream results in the density difference. At a given M , film cooling effectiveness is directly proportional to DR , however, at higher DR and lower M the effect can be reverted in the case of a leading edge. In some cases even complete shutoff of coolant to stagnation region has also been observed. Similar results are reported by Li et al. [2], Gao et al. [4] and Salcudean et al. [5].

Impingement (IMP) is employed to improve the internal cooling at the stagnation region. However, its effect on the external film cooling effectiveness is a new parameter to study. Most of the information available in the open literature [6] deals with impingement separately and its effect on the outside film cooling is rarely discussed. For the present study, a semi-elliptical model is used to investigate the influence of the inlet flow condition effects on the film cooling effectiveness. Typical ranges of blowing ratio ($M = 0.5, 1.0, \text{ and } 1.5$) and density ratio ($DR = 1.0, 1.5, \text{ and } 2.0$) were investigated. The PSP measurement technique is used to obtain the detailed film cooling effectiveness distributions. In addition, the RKE model is used to understand the internal flow pattern.

EXPERIMENTAL APPROACH

Experiments have been accomplished in a low-speed suction type wind-tunnel facility as shown in Fig. 1. The cross-section of the test section is 76.2 cm x 25.4 cm. Mainstream flow is achieved using an induction fan on the downstream. The mainstream flow enters the test section through a converging section that has a fine mesh screen at the inlet. A bar grid (1.27 cm) is installed between the converging duct and test section producing a turbulence intensity of 7% with an integral length scale of 1.7 cm at the downstream location. The main flow is fixed at a Reynolds number of 102,446 based on the oncoming velocity and the semi-cylinder diameter. The inlet velocity is measured by a pitot-static probe and found to be 20.89 m/s.

The test model is an elliptical leading edge with an after body and has a major radius of $1.5R$ ($R = 38.1 \text{ mm}$). The model is placed 76.2 cm downstream of the turbulence grid. Figure 2 shows the LE design that includes three rows of cylindrical film cooling holes. Row 1 is located at the stagnation line (0°) where the mainstream air directly hits the LE model. Rows 2 and 3 are located at $s/d = 6.7$ ($\sim \pm 30^\circ$) and rows 4 and 5 referred as gill film holes (GH) are located at $s/d = 17$ ($\sim \pm 60^\circ$). LE cooling holes (row 1~3) are oriented in the radial direction and orthogonal to the local mainstream flow direction whereas the gill film holes are in the streamwise direction. All these holes are arranged inline pattern with an inclined angle of 30° relative to the surface. Each row has 15 holes with a hole-to-hole pitch of $4d$ in the radial direction (z). The model has the flexibility to use either IMP OFF or IMP ON (Fig. 3) inlet conditions. Internal impingement hole plate is kept at a fixed distance of 31.7 mm from the hole exit to the target stagnation point. Film cooling holes and impingement cooling holes are staggered. The details of film cooling hole and impingement cooling hole configurations are summarized in Table 1.

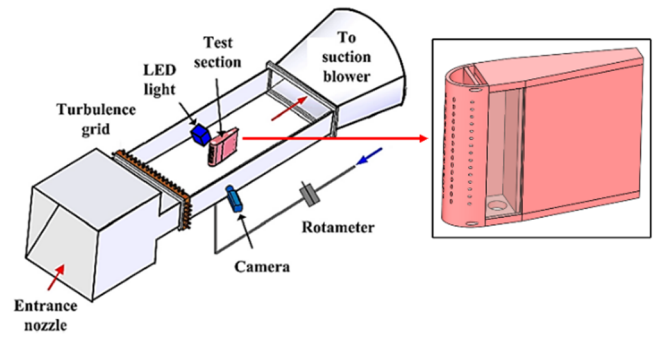


Figure 1. Experimental Setup

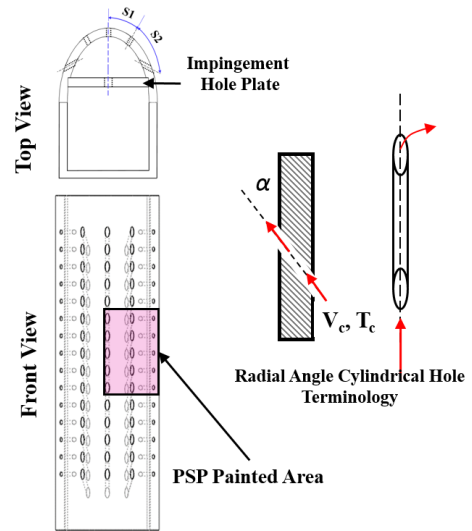


Figure 2. Leading edge model and hole configuration

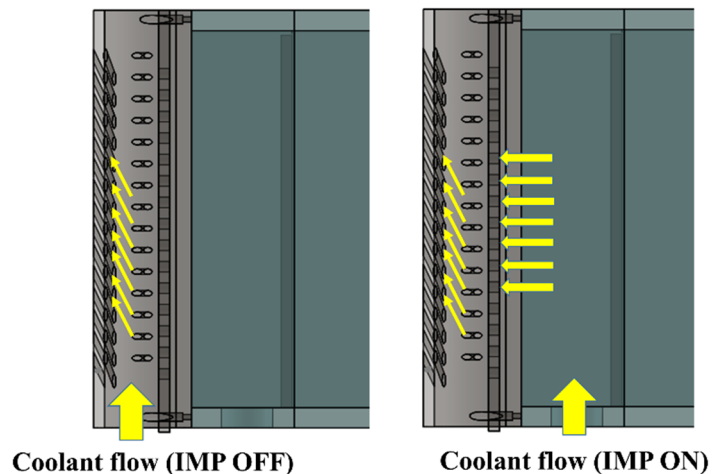


Figure 3 Coolant supply arrangements

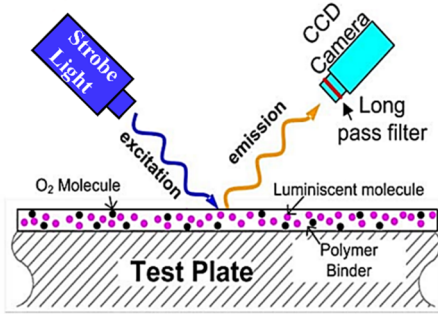
Table 1. Hole Configuration

Parameters	LE	GH	IMP
Hole diameter, d (cm)	0.32	0.32	0.62
Hole to hole spacing, P (cm)	4d	4d	4d
Hole length to diameter ratio, (L/d)	4.73	4.73	1.5
Angle to surface, α (deg)	25	32.5	0
Streamwise angle, β (deg)	90	0	-
Row Spacing (from stag. line), (cm)	2	4	-
Plate thickness, t (cm)	0.95	0.95	0.95
IMP to stag. line distance, l (cm)	-	-	3.17

EXPERIMENTAL TECHNIQUE

PSP Measurement Technique

Principle. Film cooling effectiveness over a surface can be measured using PSP based on heat and mass transfer analogy. PSP is comprised of photoluminescent molecules and an oxygen-permeable polymer binder, both dissolved in a solvent. The paint used here is UniFIB UF470-750 from ISSI Inc. When the paint is excited by a strobe light source with a certain wavelength, then the luminescent molecules in the paint emit photons at a wavelength around 650 nm as a relaxation from an excited state to their ground state. The emission intensity of painted surface is recorded using A Cooke Sencicam CCD camera with a long pass filter. With the presence of oxygen molecules, luminescent molecules interact and transmit energy to oxygen molecules during their return to the ground state; this is known as oxygen quenching. In this radiation-less deactivation process, the intensity of the emitted light decreases with an increase in the concentration of oxygen (partial pressure) and this phenomenon serves as working principle for PSP. A typical PSP system is depicted in Fig. 4.

**Figure 4 PSP working principle**

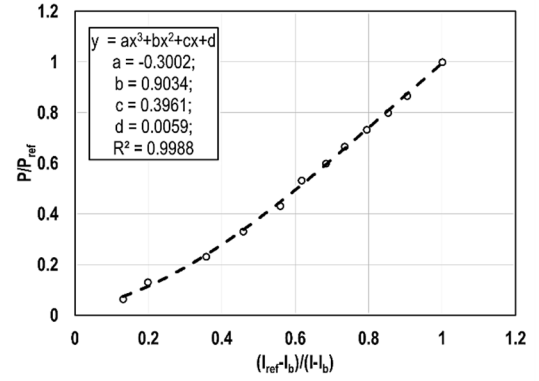
Calibration. A CCD camera is used to record the emitted light intensity, then a relation between the partial pressure of oxygen (for the constant concentration of oxygen in the ambient air, this is equivalent to the partial pressure of air) and the emission intensity can be established by calibration.

The CCD camera was set to capture 200 grey-scale images at each pressure to reduce the measurement noise. The emission intensity was then calibrated for a range of known pressures expected during the experiments. Thus, the partial pressure of oxygen adjacent to the painted surface was correlated

to the surface emission intensity by a polynomial fitting curve using equation [Eq. 1].

$$\frac{I - I_{blk}}{I_{ref} - I_{blk}} = f\left(\frac{P_{O_2}}{P_{O_2,ref}}\right) \quad (1)$$

The emission intensity I corresponds to a specific pressure, recorded during the calibration. The reference intensity, I_{ref} was the measured intensity under the reference pressure $P_{O_2,ref}$ (ambient pressure) and I_{blk} is the intensity associated with the black images recorded under the dark room condition considered as the background noise of the camera. The calibration curve used in this study is presented in Fig. 5.

**Figure 5 PSP Calibration Curve**

Film Cooling Effectiveness. To calculate film cooling effectiveness, two different coolants are required to inject independently. Generally, air is used as one of the coolants while another coolant can be any one of the oxygen-free foreign gas. As the foreign gas is injected, it interacts with the molecules on the PSP coated surface resulting in variation of the emitted intensity. The emitted intensity also measured from the air case. From the difference in emitted intensity (i.e. partial pressure of oxygen) of injected air and foreign gas, film cooling effectiveness can be computed. Based on the heat and mass transfer analogy [7], film cooling effectiveness can be expressed as

$$\eta_{aw} = \frac{T_m - T_{aw}}{T_m - T_c} \approx \frac{C_m - C_w}{C_m - C_c} \approx \frac{C_{O_2,air} - C_{O_2,fg}}{C_{O_2,air} - C_{O_2,c}(\approx 0)} \quad (3)$$

$$\eta_{aw} = 1 - \frac{C_{O_2,fg}}{C_{O_2,air}} \quad (4)$$

Replacing concentration terms with corresponding oxygen partial pressures yields the final form:

$$\eta_{aw} = 1 - \frac{1}{\left[\left(\frac{P_{O_2,air}/P_{O_2,ref}}{P_{O_2,fg}/P_{O_2,ref}} - 1\right) \frac{W_{fg}}{W_{air}} + 1\right]} \quad (5)$$

where $CO_{2,air}$ and $P_{O_2,air}$ are the oxygen concentration and partial pressure with air injection, $CO_{2,fg}$ and $P_{O_2,fg}$ are the oxygen concentration and partial pressure with foreign gas injection, W_{air}

is the molecular weight of air, and W_{fg} is the molecular weight of the foreign gas.

UNCERTAINTY ESTIMATION

Uncertainty estimations have been performed based on the method of Kline and McClintock [8]. The uncertainty in mainstream inlet velocity measurement is found to be maximum 1% and 6% for coolant mass flow rates at the lowest one. For the film cooling effectiveness, the uncertainty based on a 95% confidence level is estimated to be 15%, 3.9%, 1.7% and 0.7% at $\eta = 0.1, 0.3, 0.5,$ and 0.7 accordingly.

RESULTS AND DISCUSSIONS

The leading edge model includes two configurations: IMP OFF and IMP ON. The density ratio varies from 1.0, 1.5 to 2.0, while the blowing ratio varies from 0.5, 1.0 to 1.5. The blowing ratio is calculated based on the mainstream velocity and the cross-sectional area of all open cooling holes. Experimental results are presented and discussed as effectiveness contour plots, span-wise averaged effectiveness plots, and area averaged effectiveness plots. Averaged effectiveness plots include film hole area where the effectiveness is very high (0.9~1.0). Due to the symmetry of the model, data are captured on the one side of the cylinder. Also, data reported (PSP painted area) are only based on the middle five holes per row due to the edge effect.

Detailed film cooling effectiveness distributions are presented in **Figs. 6-8** with IMP OFF and ON at $DR = 1.0, 1.5$ and 2.0 accordingly at the blowing ratio $M = 0.5, 1.0$ and 1.5 . The horizontal axis is s/d (along with mainstream direction) and the vertical axis is z/d (along with the span-wise direction). The stagnation row is located at $s/d = 0$ and is followed by the second row at $s/d = 6.7$. Mainstream static pressure is supposedly very high near the stagnation region, so at low blowing ratio ($M = 0.5$), nearly no coolant comes out of the stagnation row. In the downstream of the second row ($s/d > 7$), as the mainstream momentum increases, the coolant is deflected by the mainstream and the film traces become longer. When the density ratio increases from 1.0 to 2.0, the film cooling effectiveness traces become wider and cover more region in the span-wise direction. As shown in **Figs. 6-8**, for a fixed density ratio, film effectiveness increases with increasing blowing ratio for both impingements OFF and ON. At low blowing ratio ($M = 0.5$), the coolant trace from second row at $DR = 2.0$ is lower than $DR = 1.0$. This is because of the insufficient momentum of heavier coolant. As there is nearly no coolant coming out from the stagnation row, it is inappropriate to use a low blowing ratio in this design. At high blowing ratios ($M = 1.0$ and 1.5), the effectiveness of $DR = 2.0$ is higher than $DR = 1.0$. The reason is that, for a given blowing ratio, the coolant momentum decreases when density increases, and the jet has a higher tendency to adhere to the leading edge surface which greatly benefit the jet from the stagnation row to travel almost entire region. Based on Fig. 6-8, it can be seen that the IMP ON inlet condition helps to achieve relatively higher cooling effectiveness and uniform coverage.

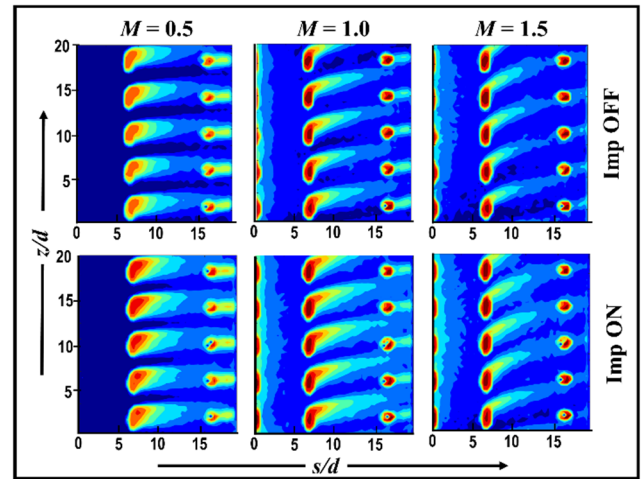


Figure 6. Film cooling effectiveness contours for $DR = 1.0$

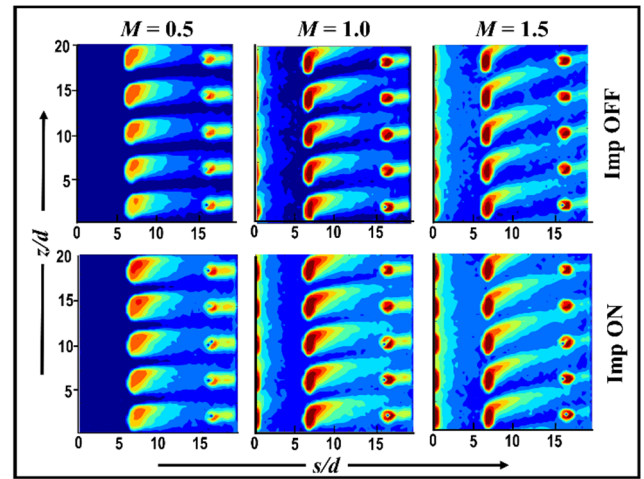


Figure 7 Film cooling effectiveness contours for $DR = 1.5$

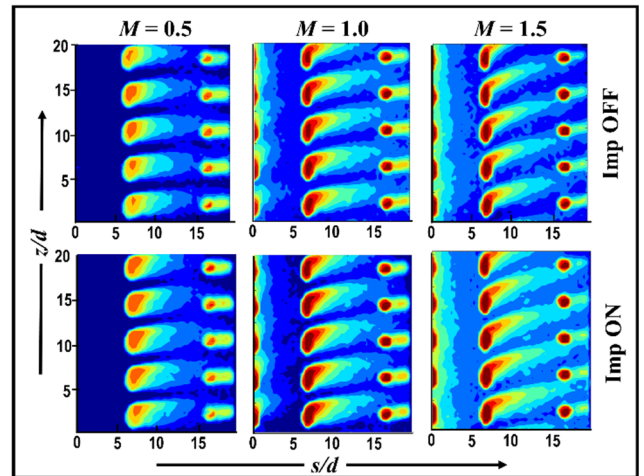


Figure 8 Film cooling effectiveness contours for $DR = 2.0$

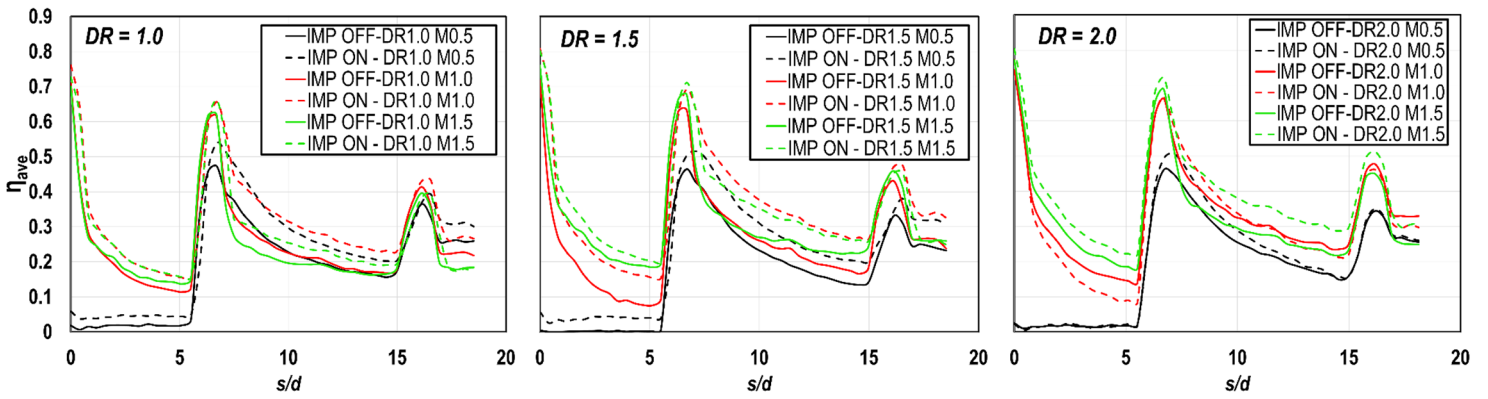


Figure 9 Spanwise-averaged film cooling effectiveness for $DR = 1.0, 1.5$ and 2.0

Spanwise average film cooling effectiveness is presented in **Fig. 9** and area-averaged film effectiveness is calculated for total 18 cases with $0 < s/d < 18$ and $0 < z/d < 20$, as shown in **Fig. 10**. $M = 0.5$ is not effective for leading edge film cooling with cylindrical holes. The effect of the inlet flow condition can be clearly observed for any fixed density ratio. Overall, IMP ON provides significantly higher span average effectiveness values compare to the IMP OFF condition. However, a very minimum difference is observed for $DR=2.0$ at $M=1.0$.

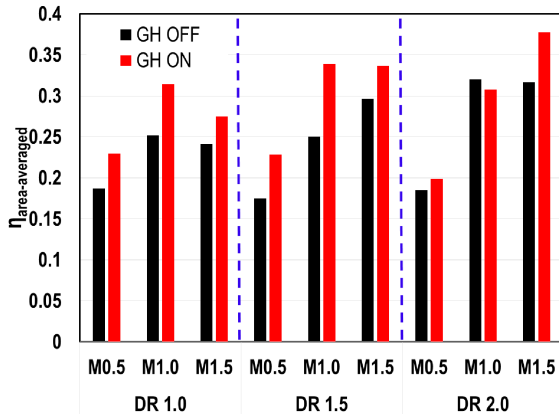


Figure 10. Area-averaged film cooling effectiveness

COMPUTATIONAL APPROACH

Computational simulations have been performed using a commercial code ANSYS FLUENT 18.0. For grid generation, both unstructured and structured meshes are employed using ICEM CFD. Unstructured meshes are generated near the leading edge region while structured ones are in the rest of the part to simulate the overall wind tunnel environment. A mesh interface is used between two types of meshes. There are 20 prism layers in the walls of leading edge, cooling holes and plenum, with y^+ value less than unity. A total number of 11.0 million for IMP OFF and 11.7 million for IMP ON grids is selected based on the grid independence test. Mesh elements are shown for GH ON condition in **Fig.11**. The RKE turbulence model and the SIMPLE method are used. The fluid is defined as incompressible ideal gas, and its properties are temperature dependent. The convergence criteria of all the simulations were set to the residual values of order 10^{-6} .

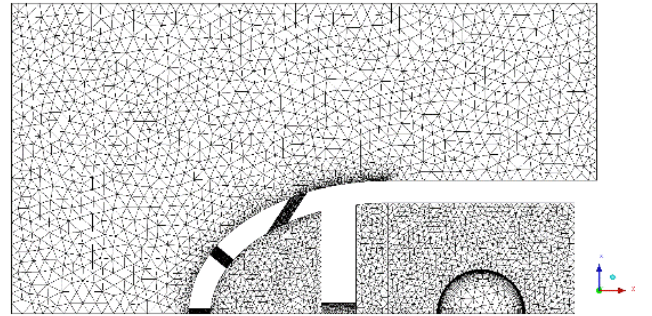


Figure 11 Mesh elements for IMP ON condition

The case for $DR = 2.0$ at $M = 1.5$ is selected to run the simulation. The mainstream temperature is 296K. The coolant temperature is 148K and the coolant turbulence intensity is 5%. Simulated results are presented in **Fig. 12** as velocity field (mid-span and symmetric plane), path lines and film effectiveness. Coolant path lines are colored by dimensionless temperature (θ).

$$\theta = \frac{T_{\infty} - T}{T_{\infty} - T_c} \quad (6)$$

The influence of the inlet flow condition on the coolant distribution inside the plenum is clearly observed from the velocity field and the coolant path lines. Initially, the coolant temperature is the same as the inlet and then the coolant is mixed with the mainstream and the coolant temperature increases just after it ejects from the cooling holes. In the stagnation region, the predicted effectiveness for IMP OFF/ON is about the same. After the second row, the trace is wider and the effectiveness is higher for IMP ON case than IMP OFF case. Velocity fields show that the coolant velocity is relatively higher inside the plenum (near the second row inlet zone) for the IMP ON condition which led to the higher film effectiveness after that row. Additionally, different flow patterns are also observed inside the plenum for different inlet conditions, as expected. **Figure 11** shows comparisons of CFD and PSP in terms of spanwise averaged film cooling effectiveness. Generally, results from CFD are in good agreement with PSP data. The difference is about 10% to 20%.

SUMMARY

In this paper, film cooling experiments were performed on an elliptical leading edge model comparing two cooling configurations, at three blowing ratios, $M = 0.5, 1.0$ and 1.5 and three density ratios $DR = 1.0, 1.5$ and 2.0 at a turbulence level of 7%. The cooling configurations consist of three-row arrangements of cylindrical holes with gill film holes. Film cooling effectiveness was measured with IMP OFF and ON using PSP measurement technique.

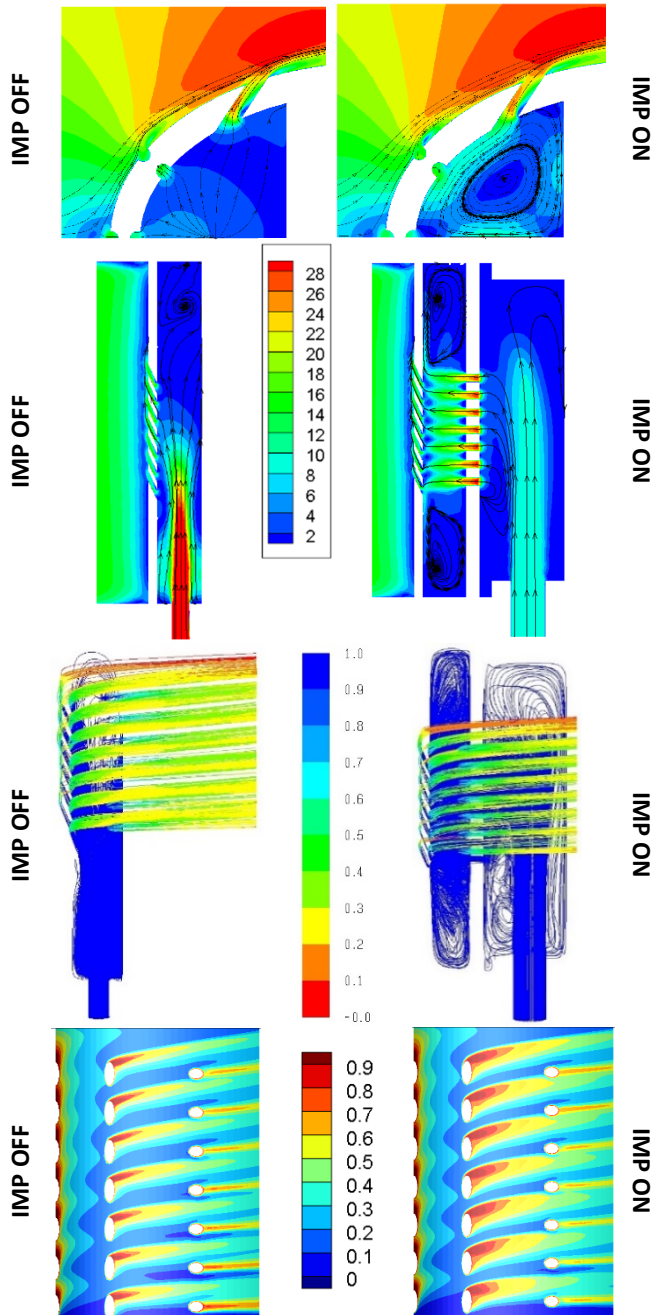


Figure 12 Velocity (m/s) Field (mid-span and symmetric plane) (upper two), Path Lines (middle one) and film effectiveness (lower one) for $DR = 2.0$ and $M = 1.5$

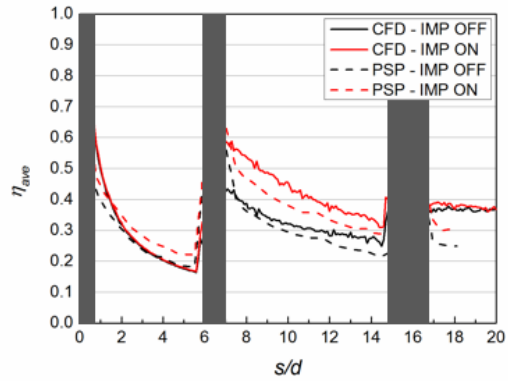


Figure 13 Spanwise averaged effectiveness comparison for $DR = 2.0$ and $M = 1.5$

Overall, IMP ON condition was found to be the best case over the IMP OFF configuration. Internal flow conditions were also investigated using RKE turbulence model. Computational results were found to be in good agreement with the experimental database, especially, for the IMP OFF case.

ACKNOWLEDGMENTS

The authors gratefully acknowledge Fulbright Scholarship support for Shamsul Qureshi and the Marcus Easterling endowment fund for funding the study. The authors also acknowledge the support of Texas A&M University Supercomputing Facility for the simulation works.

REFERENCES

- [1] C. Falcoz, B. Weigand, P. Ott, 2006, "A comparative study on showerhead cooling performance," *International J. of Heat and Mass Transfer* 49 (2006) 1274–1286.
- [2] Li, S.J, Yang, S.F. and Han J. C., 2013, "Effect of Coolant Density On Leading Edge Showerhead Film Cooling Using PSP Measurement Technique," *ASME J. of Turbomach.* Vol. 136, pp. 051011.
- [3] Han, J.C., Dutta, S., and Ekkad, S. V., 2001, "Gas Turbine Heat Transfer and Cooling Technology, Taylor & Francis, New York, 2001, p. 21.
- [4] Gao, Z. and Han, J.C., 2009, "Influence of Film-Hole Shape and Angle on Showerhead Film Cooling Using PSP Technique," *J. of Heat Transfer*, Vol. 131, pp. 061701.
- [5] Salcudean, M., Gartshore, I., Zhang, K., and McLean, I., 1994, "An Experimental Study of Film Cooling Effectiveness Near the Leading Edge of a Turbine Blade," *ASME J. of Turbo.* Vol.116, pp.71-79.
- [6] Jordan, C.N., Wright, L.M. and Crites, D.C., 2016, "Impingement Heat Transfer on a Cylindrical, Concave Surface With Varying Jet Geometries," *ASME. J. Heat Transfer.* Vol. 138, pp. 122202.
- [7] Han, J.C., and Rallabandi, A. P., 2010, "Turbine Blade Film Cooling Using PSP Technique," *Frontiers in Heat and Mass Transfer*, Vol. 1, No.1, pp. 1–21.
- [8] Kline, S., and McClintock, F., 1953, "Describing Uncertainties in Single-Sample Experiments," *Mechanical Engineering*, 75(1), pp. 3 – 8.